Available online at www.sciencedirect.com
ScienceDirect
Materials Letters 61 (2007) 3833–3836
materials letters
www.elsevier.com/locate/matlet

X-ray absorption fine structure combined with X-ray fluorescence spectrometry Part 18. Tin site structure of Pt–Sn catalyst

Yasuo Izumi [a,*], Dilshad Masih [a], Eric Roisin [b], Jean-Pierre Candy [b], Hajime Tanida [c], Tomoya Uruga [c]

[a] *Interdisciplinary Graduate School of Science and Engineering, Tokyo Institute of Technology, Nagatsuta 4259-G1-16, Midori-ku, Yokohama 226-8502, Japan*
[b] *Laboratoire de Chimie Organometallique de Surface, UMR CNRS-CPE 43 bd du 11 Novembre 1918, F-69616 Villeurbanne, France*
[c] *Japan Synchrotron Radiation Research Institute, Kohto 1-1-1, Sayo 679-5198, Japan*

Received 13 May 2006; accepted 19 December 2006
Available online 8 January 2007

Abstract

Sn Kα_1-detecting Sn K-edge XANES spectrum was successfully measured for Pt–Sn/SiO_2 catalyst (2.5 wt.% Pt, Sn/Pt atomic ratio 1.0) in the energy resolution 5.0 eV using Rowland-type fluorescence spectrometer equipped with Ge(13,13,13) bent crystal. The steeper, more clearly resolved XANES spectrum thus obtained could be compared quantitatively to theoretical XANES spectra generated by *ab initio* calculations for thirteen plausible Pt–Sn site models (alloy, adsorbed Sn, and mixture models). This spectral simulation suggested that fluorescence-detecting XANES is a simple method to judge the plausible site structure without detailed spectral analyses. The comparison supported an adsorbed Sn site model structure on highly dispersed Pt[–Sn] nanoparticles on SiO_2.

Keywords: Catalysts; Characterization methods; Nanocomposites; X-ray techniques; XANES

1. Introduction

Pt–Sn binary catalysts have been widely investigated for selective hydrogenation of unsaturated aldehydes [1–3], dehydrogenation of alkanes [4–7], and reforming [5,8]. The presence of tin favors the selective hydrogenation of carbonyl group, the formation of unsaturated olefins rather than smaller alkanes, and suppresses coke formation. In this work, the feasibility of the tin site structure study is demonstrated by Sn K-edge XANES (X-ray absorption near-edge structure) combined with X-ray fluorescence spectrometry for Pt–Sn binary catalyst. The core-hole lifetime broadening is serious at higher-energy absorption edge XANES [9]. Because obtained high energy-resolution Sn Kα_1-detecting Sn K-edge XANES spectrum was sharper (more resolved), it could be quantitatively compared to theoretical XANES generated by *ab initio* calculations.

2. Experimental

An aqueous slurry of $Pt^{II}(NH_3)_4(OH)_2$ was mixed with silica (Degussa, 200 $m^2\ g^{-1}$) [4]. After filtration, obtained powder was calcined and then in H_2 at 673 K (Pt/SiO_2). Sn(n-C_4H_9)$_4$ was introduced to Pt/SiO_2 in H_2 (3.0 kPa) at 373 K (Pt–Sn/SiO_2). Then, it was treated in H_2 at 673 K and sealed in Pyrex glass cell. The Pt loading was 2.5 wt.% and Sn/Pt atomic ratio was 1.0. The amount of Sn supported was determined by elemental analysis and doubly checked by measuring unreacted Sn(n-C_4H_9)$_4$ by GC [4].

X-ray measurements were carried out at the undulator beamline 10 XU and 37 XU in SPring-8. Storage ring energy was 8.0 GeV and the current was 100–71 mA. Si(111) double crystal monochromator was used. All the X-ray spectra were measured at 290 K. The Sn Kα_1 fluorescence was analyzed by a Rowland-type spectrometer [10] equipped with a Johansson-type Ge(13,13,13) crystal (Saint-Gobain, Rowland radius 220 mm) and NaI(Tl) scintillation counter. The Sn Kα_1 emission

* Corresponding author. Tel./fax: +81 45 924 5569.
E-mail address: izumi.y.ac@m.titech.ac.jp (Y. Izumi).

0167-577X/$ - see front matter © 2006 Elsevier B.V. All rights reserved.
doi:10.1016/j.matlet.2006.12.077

spectra were measured with the excitation energy at 29235.0 eV. The spectrometer was tuned to the Sn Kα$_1$ peak and Sn K-edge XANES spectrum was measured. The undulator gap and the parallelism of the monochromator crystals were optimized to maximize the X-ray beam flux at each data point.

Sn Kα$_1$-selecting Sn K-edge XANES was compared to that theoretically generated by FEFF8.2 in self-consistent field and full multiple scattering calculation modes [11]. The Hedin–Lundqvist self-energy was used for energy-dependent exchange-correlation potential. The calculated potential was corrected by adding a constant shift to "pure imaginary optical potential". Because the Sn Kα$_1$-selecting XAFS was measured under the condition that the energy resolution of fluorescence spectrometer (5.0 eV) was smaller than the core-hole lifetime width Γ_K of Sn K level (8.49 eV [9]), the energy shift to "pure imaginary optical potential" was set to −4.0 eV. The XANES simulation with this method was already successful for tin metal [10]. The goodness of simulation was evaluated based on *R*-factor ($R_f=\int|\chi^{obs}(k)-\chi^{calc}(k)|^2dk/\int|\chi^{obs}(k)|^2dk$). A code XDAP 2.1.2 was used for the EXAFS analyses [12]. The phase-shift and amplitude parameters were extracted from EXAFS spectrum of SnO_2 powder for Sn–O bond (2.053 Å) and theoretically generated using FEFF8.2 [11] for Sn–Pt bond.

3. Results and discussion

In the Sn Kα$_1$-selecting Sn K-edge XANES spectrum (Fig. 1exp-f), the first intense peak at 29206.3 eV (Table 1) became sharper and absorption edge at 29200.3 eV became steeper compared to corresponding XANES measured in transmission mode (exp-t). When the high-energy resolution spectrum exp-f was convoluted using a Lorentzian of Γ_K for Sn, transformed data (Fig. 1exp-f-c) resembled spectrum exp-t. The Sn Kα$_1$-selecting XANES became deconvoluted data of conventional XANES. The obtained Sn–O (2.108±0.007 Å) and Sn–Pt distances (2.713±0.006 Å) for Sn K-edge EXAFS were within the range reported: 2.053–2.224 Å [13] and 2.63–2.80 Å [4,14–16], respectively. Following XANES simulation was performed within this range of bond distances.

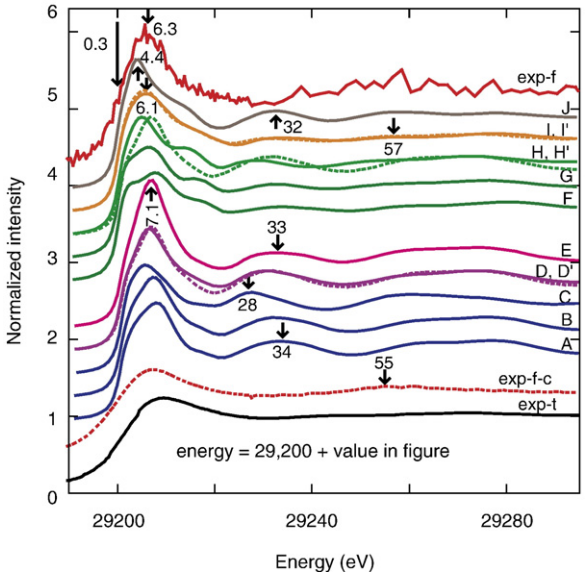

Fig. 1. Normalized Sn K-edge XANES spectra for Pt–Sn/SiO_2 catalyst by the selective detection of Sn Kα$_1$ (exp-f) or in transmission mode (exp-t). The data exp-f was convoluted to be exp-f-c using a Lorentzian of 8.49 eV (width). Sn K-edge XANES spectra generated by FEFF for models A–I (spectra A–I, respectively). Dotted spectra D′ and H′ are for Sn site in the second layer in models D and H, respectively. Data J is the average theoretical spectrum for Sn site model inside the Pt bulk (33%) and of $Sn^{II}O$ (67%).

Table 1
Energy values of absorption edge and intense peak above the edge for experimental XANES for Pt–Sn/SiO_2 catalyst and theoretical XANES generated for various models

	Energy (eV)		
	Absorption edge	Intense peak	R_f compared to exp-f spectrum (%)
(A) Experimental			
Kα$_1$-selecting	29,200.3	29,206.3	
Transmission mode	29,201.1	29,209.8	
(B) Theoretical			
Model A	29,200.6	29,208.3	2.71
Model B	29,200.7	29,207.5	2.78
Model C	29,200.9	29,206.1	2.63
Model D (surface)	29,200.7	29,206.7	2.44
(second layer)	29,200.8	29,207.4	2.60
Model E	29,200.7	29,207.1	2.33
Model F	29,200.2	29,208.1 (29,203.5)	2.20
Model G	29,200.2	29,206.7 (29,203.3)	1.86
Model H (surface) [a]	29,200.3	29,205.3	1.80
(second layer)	29,200.7	29,207.0	2.91
Model I [a]	29,200.2	29,206.1	1.27
Model J	29,199.9	29,204.4	1.47

[a] Reasonable models for Sn site for Pt–Sn/SiO_2 catalyst.

Sn Kα$_1$-selecting XANES was simulated based on models A–I (Fig. 2). Alloy Pt–Sn models A–E were based on face-centered cubic packed Pt cluster within 7.0 Å from the central X-ray absorbing Sn atom. The (111) face exposure was assumed. One third of surface Pt atoms were replaced with Sn atoms in model B. The calculated Sn K-edge XANES spectra (Fig. 1A and B) resembled each other. The substitution of neighboring Pt with Sn negligibly affected the XANES. In spectrum C for model C, XANES profile was similar to those for spectra A and B, however, whole the pattern shifted toward the lower energy side. The intense peak above the absorption edge and next broad peak shifted by −1.4 to −2.2 and −5 to −6 eV, respectively.

One third of Pt atoms were replaced with Sn atoms both at surface and in bulk for model D. The spectrum D (solid line) calculated for the surface Sn site was the intermediate on going from spectrum A/B to C based on the energy values of absorption edge and post-edge peaks and their relative intensity. Spectrum D′ (dotted line) for the Sn site in the second layer resembled D (solid line) for surface Sn site. The post-edge peak at 29231 eV either for surface or bulk Sn site in model D was not similar to exp-f.

Three-fold oxygen atoms (three atoms) were bonded to the central Sn atom in model E (Fig. 2). Common broad peak for spectra A, B, C, D, D′, and E at 29,228–29,234 eV did not resemble that of exp-f (R_f=2.33–2.78%, Table 1). Alloy models A–E were rejected as the Sn site model in Pt–Sn/SiO_2 catalyst.

For isolated adsorbed Sn model F, the intense peak above the absorption edge split into two and was broader (Fig. 1F) compared to exp-f. One third of surface was adsorbed with Sn atoms in adsorbed Sn site model G. Generated spectrum (Fig. 1G) was essentially identical

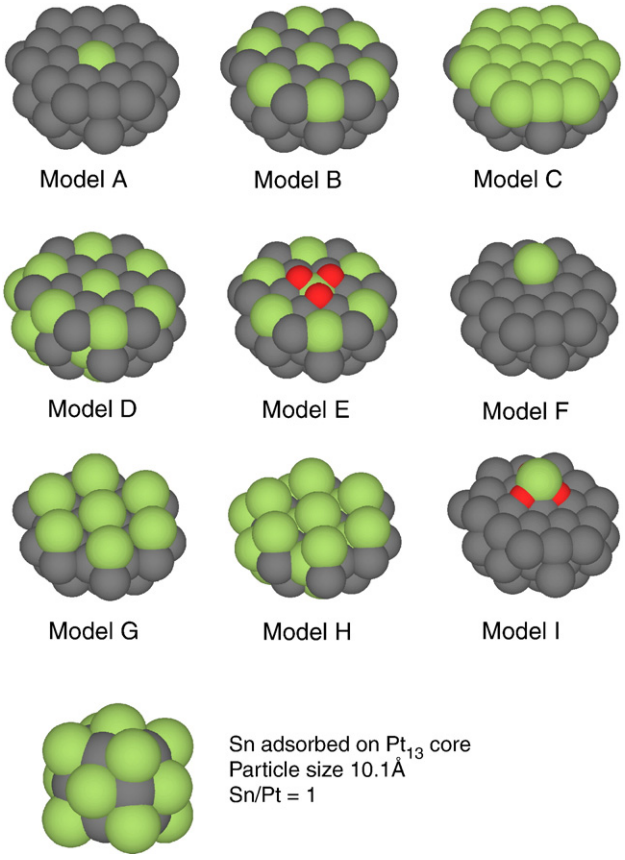

Fig. 2. Sn local site models on/in Pt[–Sn] nanoparticles. Gray: Pt, green: Sn, and red: O atoms. Sn–Pt bond distance was assumed to be equal to Pt–Pt bonds (2.775 Å) in models A–E and for bulk section in model H. The Sn–Pt distance (surface) in models F–I was varied within 2.63–2.80 Å and typically set to 2.713 Å. The Sn–O and Pt–O distance in models E and I was varied within 2.053–2.224 Å and typically set to 2.108 Å. In model I′, the Sn–Pt distance was elongated to 2.800 Å.

with F. The addition of adsorbed Sn on neighboring Pt negligibly affected the XANES pattern.

Further, one third of the bulk section in model G was substituted with Sn sites (Fig. 2H). For the surface Sn site (Fig. 1H, solid line), the intense peak at 29,205.3 eV became stronger compared to that in spectrum F or G. The post-edge pattern beyond 29,220 eV was relatively flat. A weak peak appeared at 29,258 eV similar to the broad peak for exp-f (29,055 eV). Theoretical spectrum for the Sn site in the second layer in model H (Fig. 1H′, dotted line) was more similar to spectrum A, B, D, D′, or E. Because experimental XANES spectrum is the statistical average for all the Sn sites in sample, model H was acceptable as the Sn catalyst site model if the contribution of adsorbed Sn sites was predominant, *i.e.* ultimately high metal dispersion of Pt–Sn nanoparticles, *e.g.* adsorbed Sn model on the Pt_{13} core (Fig. 2, bottom).

Three-fold oxygen atoms (three atoms) were added to model F (model I). Note that to simplify, adsorbed Sn site was only one in model I because the contribution of adsorbed Sn atoms on neighboring Pt sites was negligible to XANES (Fig. 1F and G). Theoretical XANES for the model I resembled most exp-f (exp-f-c) (R_f=1.27%) based on the intensity and broadness of whiteline peak and post-edge peak (Table 1). When the Sn–Pt bond distance was elongated to 2.80Å (model I′) from 2.713Å (model I), the calculated spectrum changed negligibly (Fig. 1I′ and I).

Model I can be acceptable when surface density of adsorbed Sn was greater and core Pt particle size was small enough to enable experimental atomic ratio Sn/Pt 1.0, *e.g.* adsorbed Sn model on the Pt_{13} core (Fig. 2, bottom). The structure I was consistent with EXAFS curve fit results (N(Sn–O) of 3.0±0.5 and N(Sn–Pt) of 4.0±1.0). Because theoretical Sn K-edge XANES profile was insensitive to the presence of oxygen atoms adsorbed (Fig. 1B *versus* E; F *versus* I), the presence of adsorbed oxygen(s) could not be judged in model H. Similar adsorbed Sn model was reported on small metal cluster inside zeolite cage [6]. For Pt–Sn/SiO_2 (1.4 wt.% Pt, Sn/Pt atomic ratio 1.0), average metal particle size was 19 Å and 44% of surface Sn species and 56% of alloy $PtSn_x$ species were reported [5]. The surface Sn species may correspond to adsorbed Sn sites in model H or I.

Finally, mixed multiple phase model was considered. A central Sn atom site inside Pt particle bulk [N(Sn–Pt)=12] and Sn site in $Sn^{II}O$ [N(Sn–O)=4] were mixed with the ratio 1:2 [resultant N(Sn–Pt)=4 and N(Sn–O)=2.67]. In the obtained spectrum (Fig. 1J), the energy values of absorption edge, the first strong peak, and a post-edge peak (29,232 eV) were inconsistent with exp-f (exp-f-c) (Table 1) (R_f=1.47%). Thus, mixed phase model of alloy and Sn oxide sites was inappropriate.

The whiteline peak energy in spectrum exp-f corresponded to that for $Sn^{II}O$. The absorption edge energy was relatively constant for models A–I (Table 1) comparable to 29,200.3 eV for Pt–Sn/SiO_2 (Fig. 1exp-f). Thus, partial electron transfer was suggested from Sn to Pt. The extent of electron transfer was greater when the Sn site was incorporated in alloy, *e.g.* models A–E and bulk section of model H (29,200.6–29,200.9 eV) compared to those for adsorbed Sn sites in models F, G, H, and I (29,200.2–29,200.3 eV) [7].

4. Conclusions

Sn $K\alpha_1$-selecting Sn K XANES spectrum was successfully obtained at highly brilliant undulator beamline in SPring-8 combined with fluorescence spectrometry, with the energy resolution of 5.0 eV for Pt–Sn/SiO_2 catalyst. The Sn content was as small as 1.5 wt.%. The selective XANES was compared to theoretical XANES for various Pt–Sn alloys, adsorbed Sn sites, and mixture models. Adsorbed Sn site models on ultimately dispersed Pt[–Sn] core particles were demonstrated to be appropriate for the Pt–Sn/SiO_2 catalyst.

Acknowledgements

X-ray experiments were performed under the approval of SPring-8 Program Review Committee (2004A0122-NX-np, 2003B0386-NXa-np). This work was supported from the Grant-in-Aid for Scientific Research (17550073) and the Priority Area “Molecular Nano Dynamics” (432-17034013) from the Ministry of Education, Culture, Sports, Science, and Technology.

References

[1] S. Recchia, C. Dossi, N. Poli, A. Fusi, L. Sordelli, R. Psaro, J. Catal. 184 (1999) 1–4.
[2] A. Huidobro, A. Sepulveda-Escribano, F. Rodriguez-Reinoso, J. Catal. 212 (2002) 94–103.
[3] I.M.J. Vilella, S.R. de Miguel, C.S.M. de Lecea, A. Linares-Solano, O.A. Scelza, Appl. Catal., A Gen. 281 (2005) 247–258.

[4] F. Humblot, D. Didillon, F. Lepeltier, J.P. Candy, J. Corker, O. Clause, F. Bayard, J.M. Basset, J. Am. Chem. Soc. 120 (1998) 137–146.
[5] E. Roisin, J.P. Candy, J.M. Basset, D. Uzio, S. Morin, L. Fischer, J. Olivier-Fourcade, and L.C. Jumas, Hyperfines Interaction, in press, doi:10.1007/s10751-006-9247-z.
[6] S.J. Cho, R. Ryoo, Catal. Letters 97 (2004) 71–75.
[7] G.J. Siri, J.M. Ramallo-Lopez, M.L. Casella, J.L.G. Fierro, F.G. Requejo, O.A. Ferretti, Appl. Catal., A Gen. 278 (2005) 239–249.
[8] F. Epron, C. Carnevillier, P. Marecot, Appl. Catal., A Gen. 295 (2005) 157–169.
[9] M.O. Krause, J.H. Oliver, J. Phys. Chem. Ref. Data 8 (1979) 329–338.
[10] Y. Izumi, H. Nagamori, F. Kiyotaki, D. Masih, T. Minato, E. Roisin, J.P. Candy, H. Tanida, T. Uruga, Anal. Chem. 77 (2005) 6969–6975.
[11] A.L. Ankudinov, B. Ravel, J.J. Rehr, S.D. Conradson, Phys. Rev., B 58 (1998) 7565–7576.
[12] Y. Izumi, D. Masih, K. Aika, Y. Seida, J. Phys. Chem., B 109 (2005) 3227–3232.
[13] Kgaku-binran, Basic edition, 5th revision, Chemical Society of Japan, Ed, Maruzen, 2004.
[14] S. Mukerjee, J. McBreen, J. Electrochem. Soc. 146 (1999) 600–606.
[15] H.H.C.M. Pinxt, B.F.M. Kuster, D.C. Koningsberger, G.B. Marin, Catal. Today 39 (1998) 351–361.
[16] T. Inoue, K. Tomishige, Y. Iwasawa, J. Chem. Soc., Faraday Trans. 92 (1996) 461–467.